

CORRUGATED SUBSTRATE INTEGRATED WAVEGUIDE (SIW) ANTIPODAL LINEARLY TAPERED SLOT ANTENNA ARRAY FED BY QUASI-TRIANGULAR POWER DIVIDER

T. Djerafi* and K. Wu

Poly-Grames Research Center, École Polytechnique de Montréal, Montréal, QC H3T 1J4, Canada

Abstract—In this paper, a new configuration of Tapered Slot Antenna (TSA) with improved radiation pattern is proposed and studied. This antenna is designed in the form of a substrate integrated waveguide (SIW) array with respect to side lobe level constraints. For side lobe reduction, a simple quasi-triangular distribution is proposed and is accomplished uniquely by means of 3 dB power dividers. A 12-way series feed network with T -junction is designed and demonstrated. Radiation features of the antenna array are discussed to illustrate the accomplishment of a low side lobe level (-19 dB) of the array. The proposed antenna demonstrates the ability of the SIW technology to achieve a very low side lobe in a simple, compact and planar structure.

1. INTRODUCTION

In many practical system applications, such as microwave and millimeter-wave radar, communication and imaging, it is necessary to accommodate antenna in those systems design and implementation with high gain, low side lobe level (SLL) and low cross-polarisation [1, 2]. Such attractive characteristics can ensure low interference, high resolution and long range performances. This is crucial in meeting system specification. Inappropriate side lobes lead to false alarm in the use of a collision avoidance radar system for intelligent cruise control (ICC) applications. In this case, the SLL problem can lead to a dangerous situation in the tracking of vehicles [3].

To meet the preset gain requirement, simple antenna element is generally not sufficient. An appropriate antenna array must be used.

Received 19 September 2011, Accepted 6 December 2011, Scheduled 15 December 2011

* Corresponding author: Tarek Djerafi (tarek.djerafi@polymtl.ca).

In the design of such array, not only antenna element is important, but also the feeding structure presents a critical factor for achieving a specific performance. The element-to-element spacing defines the state of grating lobes while influencing the desired high gain and scan angle [5]. Of course, this spacing must be less than λ_0 (free space wavelength). In other words, the width of elements has to be narrower than λ_0 [4].

Another source that deteriorates the SLL dramatically is related to any extra-components placed on the same substrate that cause spurious radiation in broadside. These spurious radiations have less effect on the end-fire antenna [1], such as tapered slot antenna (TSA) [6]. Several TSA designs have been reported, namely: LTSA (Linearly Tapered Slot Antenna), Vivaldi (Exponentially Tapered Slot Antenna), CWSA (Constant Width Slot Antenna) and BLTSA (Broken Linearly Tapered Slot Antenna) [5–16]. It is well-known that the TSA features high gain, low VSWR, and wide bandwidth. However, antenna width reduction is necessary when it is used to form an antenna array. It has been documented that a reduced antipodal LTSA (AL TSA) antenna width is closely associated with degradation in radiation pattern, resulting in a significant problem for the design of compact TSAs [9].

Recent emerging research and development suggest that the substrate integrated waveguide (SIW) technology possesses attractive features, such as low-profile, low-weight, low-cost, easy implementation compatible with current microwave and millimetre-wave design and fabrication platforms. So far, a vast range of SIW components including filters, phase shifters, transitions, couplers, power dividers, and duplexers have been proposed and studied [19–23]. This scheme has been demonstrated for its nascent applications to a wide range of antennas and feeding networks as well as beam-forming architectures [12–16]. The radiation-lossless quality of the SIW structure presents an excellent potential to design array antenna feeds. In fact, the inherent radiation loss and/or cross-talk in microstrip technology used as array feeder greatly affects SLL, cross-polarisation and also introduces gain loss [17, 18]. This is in particular more pronounced at millimeter-wave frequencies where transmission loss and parasitic coupling are more sensitive.

In this paper, an SIW end-fire antenna array, built with simple amplitude distribution is studied and used to control the SLL. First, a corrugation is proposed for effectively reducing the width of antipodal LTSA without degrading their antenna patterns. Various critical parameters of this antenna are studied as well as design criteria of the material used are considered. Second, this antenna is used in an array to achieve higher gain. A series-feed mechanism is proposed

to achieve quasi-triangular distribution. In the proposed array feed, identical power divider is used to excite non-uniformly the antipodal array. The single element and array structure are fabricated. Measured results are presented and compared with its simulated counterparts.

2. SIW CORRUGATED ANTIPODAL LTSA

A SIW-based antipodal LTSA was demonstrated in [12]. In the antipodal version of the LTSA as shown in Fig. 1, the metallization on either side of the substrate is flared in opposite directions to form the tapered slot. When the SIW waveguide is used to feed the ALTSA, which is different from standard feed techniques, the bandwidth limitation caused by balun can be removed and, thus, wideband characteristics are indeed obtainable. The lowest operating frequency for this antenna is determined by the cut-off frequency of the SIW structure which has a high-pass characteristic. However, a mismatch problem takes place. To solve this problem, the flaring metal covers are designed in order to overlap. This overlap as shown in Fig. 1 is defined by parameter d_{com} . TSA width d_{with} should be larger than $2\lambda_r$. A degradation of radiation pattern has been observed for a narrower TSA width [9]. This degradation in the radiation pattern is a significant problem for the effective design of compact TSAs. Pattern improvement for a narrow width antenna can be achieved by using corrugation structure, which makes this technique suitable for the formation of antenna arrays where small spacing between antenna elements is needed. Corrugations are well known in the design of horn antennas in which they are used to suppress higher modes. Therefore, they guarantee the polarization pureness of antenna. A Fermi TSA antenna with a corrugation concept structure was proposed by Sugawara et al. [9] as well as Sato et al. [10], which has effectively reduced the width of tapered slot antennas without degrading their radiation patterns. This solution has theoretically been validated with the proposed SIW antipodal LTSA as shown in Fig. 1.

In this work, our SIW antipodal LTSA is optimized to work around 28 GHz. Substrate RT/Duroid 6002 with thickness b of $508 \mu\text{m}$ and dielectric constant of $\epsilon_r = 2.94$ is used. Parameters of the optimized structure are shown in Table 1.

Table 1. Dimensions of the antipodal LTSA with corrugation (mm).

a	d_{ant}	d_{com}	d_{with}	w_{slot}	d_{solt}
5	25.6	1.679	8.44	0.152	1.825

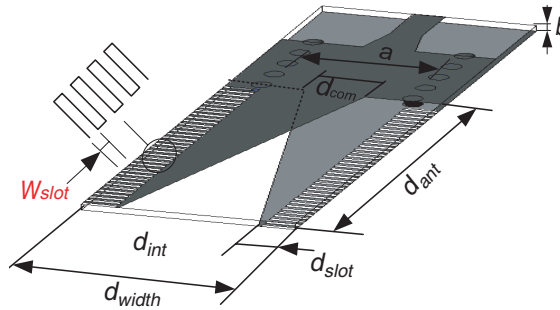


Figure 1. Corrugated antipodal linearly tapered slot array (LTSA) fed by SIW structure and microstrip to SIW transition.

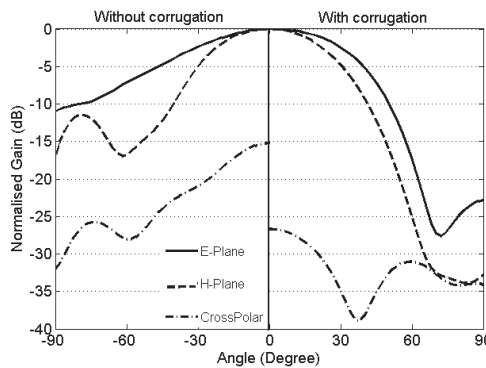


Figure 2. Simulated radiation patterns with and without corrugation obtained by HFSS at 28 GHz.

Physical dimension of the slot corrugation is constrained by our laboratory fabrication process. In fact, the smallest possible slot, feasible under this process, is $236\ \mu\text{m}$ in this work. The slot lengths are selected to be around $\lambda_r/4$, where λ_r is the wavelength in the dielectric substrate.

Figure 2 shows simulated pattern results of antennas with and without corrugation. Without corrugation, the *E*-plane pattern beamwidth is excessively large and the SLL in *H*-plane is 12 dB. Once the corrugation is used, a noticeably decreasing of 3 dB beamwidth can be observed in the *E*-plane, while the beamwidth in the *H*-plane increases. The sidelobe in the *H*-plane for this antenna is 33 dB and 32 dB in the *E*-plane. The cross-polarisation level with corrugation is found to be better than 27 dB at the frequency of design and without

corrugation is 15 dB. The latter value is however better than the non-SIW ALTSA thanks to the overlapped flaring metal.

Compared to the design in [12–14], the gain is performed without augmentation of antenna width to $2\lambda_r$, suggested in [9], the cross polarization level which is one of the drawbacks of the standard TSA is ameliorating at excellent level. The beamwidth in E plan is large, with corrugation this beamwidth is narrower which it is very important in the design of the 2D array to have pencil beam. At another level the bandwidth is larger than the antenna TSA with linear taper in [5].

To explain this improvement, simulated E -field distributions are shown in Fig. 3 along the antipodal LTSA structures with and without corrugation. Also the E -fields in the transverse plane over the radiation region are described. In the case without corrugation, the electrical field orientation at the edge of the antenna substrate is opposite to that in the antenna aperture. The corrugation structure is used to alter the phase of currents flowing along the outer edge of the substrate. It changes the orientation of the electric field at the edge of the antenna substrate. The effective antenna aperture is thus increased by the presence of the corrugation, which ensures a plane wave phase front over the antenna aperture. In standard antenna, the antipodal nature of the antenna gives rise to very high levels of cross-polarisation, particularly at high frequencies because the skew in the slot fields is close to the throat of the flare. As shown in the field distribution in the transverse view in Fig. 3, the field in the center region is more highlighted in the structure without corrugation. Out of this perturbed region, the field is parallel to the two sides of the substrate compared to the one in the antenna without corrugation which is arranged in an arc.

The impact of the slot width is verified for its dimensional variation from 6 to 12 mil. A small effect on the SLL level is observed

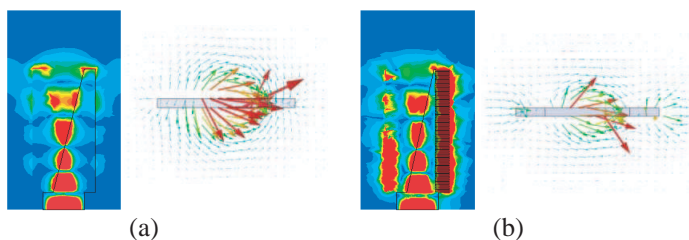


Figure 3. Simulated E -field magnitude distributions obtained by HFSS at 28 GHz, along the antenna and in transverse cut (a) antipodal LTSA without corrugation, (b) antipodal LTSA with corrugation.

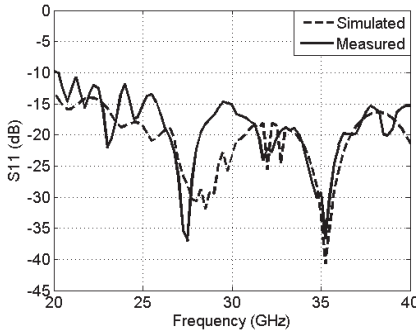


Figure 4. Measured and simulated return losses.

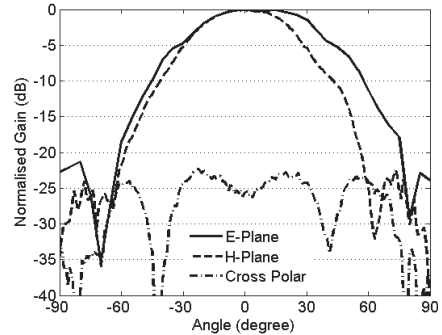


Figure 5. Measured radiation patterns at 28 GHz.

without gain degradation. For the slot depth, the variation affects the gain of the antenna by changing the effective aperture. It is possible to optimize the corrugation slot to achieve the same beamwidth in both *E*- and *H*-planes.

Simulated and measured return losses of the proposed antenna are shown in Fig. 4. The return losses are lower than 15 dB and 10 dB in the simulation and the measurement, respectively. Such degradation is probably caused by the transitions mismatch.

E-plane and *H*-plane patterns of the antenna as well as the cross-polarisations at 28 GHz are measured and shown in Fig. 5. The achieved gain is 12.2 dBi against the simulated 11.9 dBi. This difference is within the calibration-related tolerance range of the antenna reference in our anechoic chamber. The 3 dB beamwidth is 59 degree in the *E*-plane and 48 degrees in the *H*-plane and the first primary side lobe is located at -22 dB. It can be seen that the measured results are in good agreement with the simulated ones. The cross-polarisation level shows a 4 dB degradation compared to the simulated counterpart (Fig. 2).

It is noted that the TSA performances are sensitive to the thickness t and the dielectric permittivity ϵ_r of the supporting substrate. Yngvesson et al. [6] define a factor:

$$f_{\text{substrate}} = t(\sqrt{\epsilon_r} - 1) / \lambda_0 \quad (1)$$

An acceptable range for a good TSA operation is experimentally determined:

$$0.005 \leq f_{\text{substrate}} \leq 0.03 \quad (2)$$

For substrate thicknesses above the upper bound, the performance of the TSA is degraded by substrate modes. The TSA on a substrate

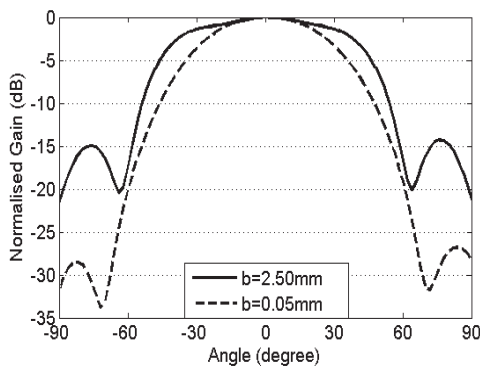


Figure 6. Simulated radiation pattern obtained by HFSS at 28 GHz corresponded to substrate thickness of 0.05 mm and 2.5 mm.

thinner than the lower bound would suffer from a decreased directivity. In the designed antenna, substrate of 2.94 relative permittivity and 0.508 mm thickness is used, which is equivalent to $f_{\text{substrate}} = 0.034$. Obviously, this value is out of the Yngvesson range. As demonstrated above, the designed antenna still works adequately in both simulation and measurement. To examine the possibility of using material out of the defined range, two different thicknesses are tested here: $b = 0.05$ mm (2 mil) and $b = 2.5$ mm ($a/2$). This is equivalent to an $f_{\text{substrate}}$ of 0.0034 and 0.101, respectively. Fig. 6 illustrates E -plane radiation patterns of the two structures selected. For the 2 mil substrate, the SLL is still low with 9 dBi of gain. For the 2.5 mm structure, the gain is 8.2 dBi and the SLL is at 15 dB. These results demonstrate the possibility to design the antipodal corrugated TSA with materials out of $f_{\text{substrate}}$ Yngvesson's range.

3. TRIANGULAR POWER DISTRIBUTION

Different types of power distribution have been used to reduce the sidelobe level of an array, such as binomial distribution, Dolph-Chebyshev distribution, triangular distribution, and Taylor distribution [4]. A power taper can be made in a parallel configuration, also called corporate feed network, in which the signal is divided at each level of the pyramid structure or can be made by either serial network [24] in which signal power is divided only at the right/ left hand side ports of individual dividers. Generally, to achieve a desired distribution, unequal power dividers with different ratio have to be used. Nevertheless, it is possible to use an identical power divider as

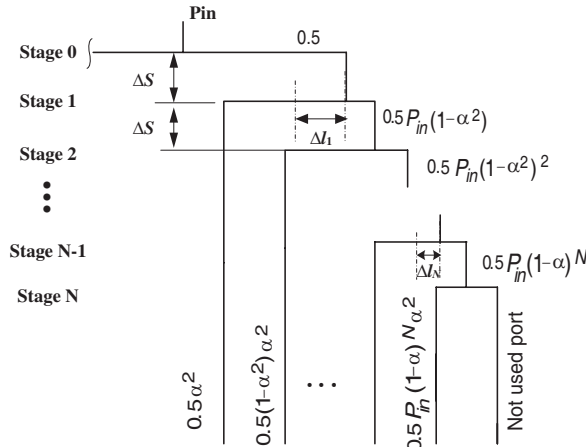


Figure 7. Half Array with the quasi triangular distribution: The feed network is composed by the cascade of power dividers with the same ratio separated by Δs , the distance Δl is used compensate the phase. The outer port is not used to define the proposed distribution.

an element in the feeding system as shown in Fig. 7. After each stage, the same power portion α^2 is directed to the outputs as shown in the figure. The power distribution is defined as:

$$P_i = P_{i-1} (1 - \alpha^2) \quad (3)$$

Figure 8 shows the amplitude at the output port versus the position for different α^2 values (0.5, 0.4 and 0.3). The excitation currents in dB as shown in Fig. 8 define a triangle while in magnitude they define convex curve (in the standard distribution, like in Taylor, the curve is concave). In case of using 3 dB power divider ($\alpha^2 = 0.5$), the power is attenuated by 3 dB after each stage to obtain (-6, -9, -12, -15, -18, -21 dB ...). The output port number can be increased by simply connecting a new power divider source to the line after N th level.

The corresponding array factor of 10 elements equally spaced at $0.5\lambda_0$ for different values of α^2 is shown in Fig. 9. The SLL level is suppressed at 20 dB and the directivity increases when α^2 decreases.

The proposed power divider is used to define the current distribution of a 10 element array. As shown in Fig. 10, the circuit is built of equal power divider T -junctions. To define the initial design parameters of the T junction with inductive matching post, a set of curves described on [25] is used. This set has been generated with the use of a FEM software package. To connect different power dividers,

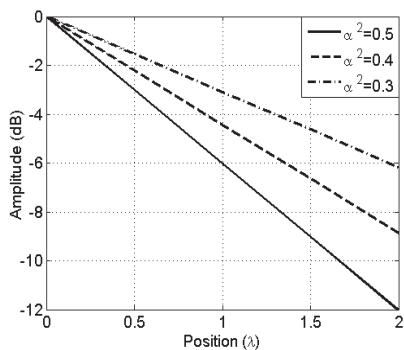


Figure 8. The proposed quasi triangular distribution as a function of the element position for different coefficient α_2 , normalized to the center element amplitude.

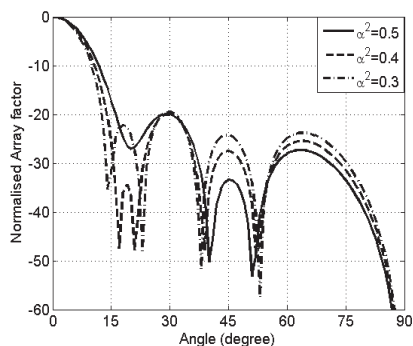


Figure 9. Array factor of 10 array elements spaced by $0.5\lambda_0$ excited by the distribution as defined in Fig. 8.

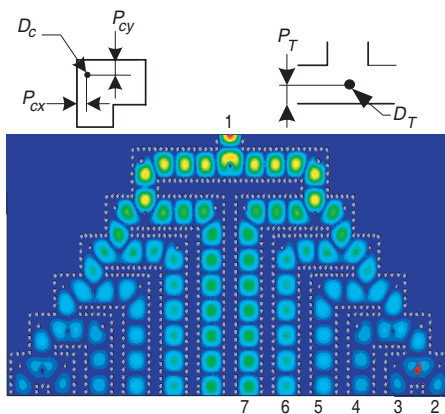


Figure 10. *E*-field magnitude distribution obtained by HFSS at 28 GHz along the power divider constructed by 3 dB *T* junctions and bends.

bends with posts are used. The initial parameters of the *T* junction are $D_T = 0.1\text{mm}$ and $P_T = 0.8\text{mm}$, and for the corner via are $D_c = 0.4\text{mm}$ and $P_{cx} = P_{cy} = 1.1\text{mm}$. To equalize phase shifts at the output ports, differential length (Δl_i) phase shifters are used. Fig. 10 presents the *E*-field distribution along the designed structure containing 3 dB-*T* power divider. As shown in the figure, the power is divided by two after each stage. The phases are thus equal at the output ports.

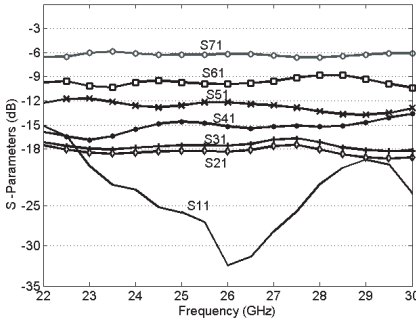


Figure 11. Couplings coefficient between the input port and the output ports as well as return loss performances.

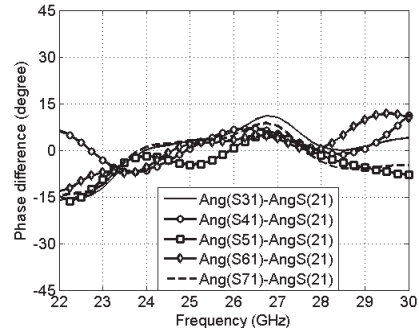


Figure 12. The phase shifts differences.

When port 1 is excited to the output ports starting by the outer port (port 2) to the central one (port 7) as shown in Fig. 10, simulated transmission coefficients in Fig. 11 are reported and compared with intending ones (namely, -6 , -9 , -12 , -15 and -18 dB). All transmission coefficients fluctuate around the ideal coupling factor in the band of 23 to 28 GHz. Over this band, the return loss is less than -20 dB. The differences of phase with port 2 as reference are shown in Fig. 12. The structure provides in-phase shift output ports with 10 degrees error from 23 to 28 GHz.

The proposed series feeder is used to feed antipodal LTSAs array. The antenna design shown in Fig. 13 is fabricated as a fully integrated feed. In principle, the last branch is not used to define the proposed quasi-triangular amplitude taper. In fact, the power ratio fed to the port 2 and 3 are the same. However, to ensure the lossless nature of this power divider, the two outputs in the outer sides are used to feed more array elements. The structure is milled by using a laser micromachining technique with very tight tolerances. The overall antenna size is of $71 \times 96 \text{ mm}^2$ involving SIW microstrip transitions.

The measured radiation pattern at 28 GHz is shown in Fig. 14 and compared to the simulated one. Both measurement and simulation are in good agreement. The gain of the main lobe is measured at 19.25 dBi with a 3 dB beamwidth of 10 degrees. There is a difference of 18.86 dB between the main beam and side lobes observed at 16 degrees. The H -plane pattern remains almost unchanged (56 degrees) compared to a single element, except a slight decrease in SSL.

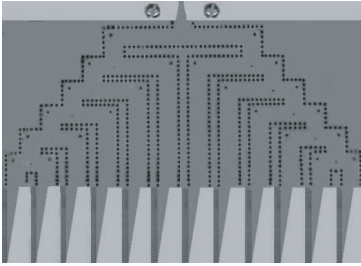


Figure 13. 1×12 antipodal LTSA array antenna feed by quasi triangular power divider.

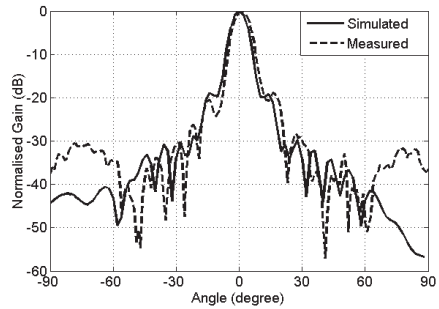


Figure 14. Simulated and measured radiation patterns of the designed 1×12 antipodal LTSAs array spaced by $0.75\lambda_0$ at 28 GHz.

4. CONCLUSION

A very compact and high performance corrugated antipodal antenna has been proposed, studied, fabricated, and measured. Measured results meet the proposed design specifications, which are in good agreement with simulated results. A wideband H -plane waveguide serial divider was designed to achieve in-phase and non-equal amplitude distributions. This power divider is used to generate the proposed simple quasi-triangular distribution and can be used to achieve various amplitude distributions. The 12-way power divider was used to feed an antipodal LTSA array antenna. Experiments at 28 GHz have confirmed the generation of the desired distribution.

ACKNOWLEDGMENT

The authors are grateful to Traian Antonescu, Steve Dubé, Jules Gauthier and Jean-Sébastien Décarie for their collaborations during the fabrication process of the structures, and also Maxime Thibault for measurements in our anechoic chamber. The authors wish to acknowledge the financial support of the Natural Sciences and Engineering Research Council of Canada.

REFERENCES

1. Bayderkhani, R. and H. R. Hassani, "Low sidelobe wideband series fed double dipole microstrip antenna array," *IEICE Electron. Express*, Vol. 22, 1462–1468, Jun. 2009.

2. Brown, D. L. and E. Rammos, "Communication satellite requirements for the year 2000 and beyond," *The 21st Century Colloquium on Satellite Antenna Technology*, 1–2, Jun. 12, 1991.
3. Kolak, F. and C. Eswarappa, "A low profile 77 GHz three beam antenna for automotive radar," *IEEE MTT-S International Microwave Symposium Digest*, 1107–1110, 2001.
4. Mailloux, R. J., *Phased Array Antenna Handbook*, 2nd edition, Artech House, 2005.
5. Yang, S., S. H. Suleiman, and A. E. Fathy, "Low profile multi-layer slotted substrate integrated waveguide (SIW) array antenna with folded feed network for mobile DBS applications," *Antennas and Propagation Society International Symposium*, 473–476, 2007.
6. Yngvesson, K. S., T. L. Korzeniowski, Y. S. Kim, E. L. Kollberg, and J. F. Johansson, "The tapered slot antenna — A new integrated element for MM wave applications," *IEEE Trans. on Microwave Theory and Tech.*, Vol. 37, No. 2, 365–374, Feb. 1989.
7. Acharya, P. R., J. Johansson, and E. L. Kollberg, "Slotline antenna for millimeter and sub millimeter wavelength," *Proc. 20th Eur. Microwave Conf.*, 353–358, Budapest, Hungary, Sep. 1990.
8. Acharya, P. R., H. Ekstrom, S. S. Gearhart, S. Jacobsson, J. F. Johansson, E. L. Kollberg, and G. M. Rebeiz, "Tapered slotline antenna at 802 GHz," *IEEE Trans. on Microwave Theory and Tech.*, Vol. 41, No. 10, 1715–1719, Oct. 1993.
9. Sugawara, S., Y. Maita, K. Adachi, K. Mori, and K. Mizuno, "Characteristics of a MM-wave tapered slot antenna with corrugated edges," *IEEE Trans. on Microwave Theory and Tech.*, 533–536, Jun. 1998.
10. Sato, H., K. Sawaya, Y. Wagatsuma, and K. Mizuno, "Broadband FDTD analysis of fermi antenna with narrow width substrate," *Int. Symp Antenna & Propagat. Society*, 261–264, 2003.
11. Venot, Y., K. Schuler, and W. Wiesbeck, "Tapered slot antenna for LTCC multilayer substrate integration in mm-wave applications," *INICA-2003, ITG-Conference on Antennas, ITGF Uchbereicht*, 49–52, Berlin, Germany, Sep. 17–19, 2003.
12. Hao, Z. C., W. Hong, J. X. Chen, X. P. Chen, and K. Wu, "A novel feeding technique for antipodal linearly tapered slot antenna array," *International Microwave Symposium*, 1641–1644, Jun. 2005.
13. Cheng, Y. J., W. Hong, and K. Wu, "Design of a monopulse antenna using a DVL TSA," *IEEE Trans. on Antennas and Propagation*, Vol. 56, No. 9, 2903–2909, Sep. 2008.

14. Li, B., L. Dong, and J.-C. Zhao, "The research of broadband millimeter-wave Vivaldi array antenna using SIW technique," *ICMMT Proc.*, 997–1000, 2010.
15. Lee, S., S. Yang, A. E. Fathy, and A. Elsherbini, "Development of a novel UWB Vivaldi antenna array using SIW technology," *Progress In Electromagnetic Research*, Vol. 90, 369–384, 2009.
16. Yang, S., E. Adel, S. Lin, A. E. Fathy, A. Kamel, and H. Elhennawy, "A highly efficient Vivaldi antenna array design on thick substrate and fed by SIW structure with integrated GCPW feed," *IEEE Antennas and Propagation Society International Symposium*, 1985–1988, 2007.
17. HALL, P. S., "Feed radiation effects in sequentially rotated microstrip patch arrays," *Electron. Lett.*, 877–878, 1987.
18. Pucel, R. A., D. Masse, and C. P. Hartwig, "Losses in microstrip," *IEEE Trans. on Microwave Theory and Tech.*, Vol. 16, No. 6, 342–350, 1968.
19. Moldovan, E., R. G. Bosisio, and K. Wu, "LW-band multiport substrate-integrated waveguide circuits," *IEEE Trans. on Microwave Theory and Tech.*, Vol. 54, 625–632, 2006.
20. Kuhlmann, K., K. Rezer, and A. F. Jacob, "Circularly polarized substrate-integrated waveguide antenna array at Ka-band," *Proceedings of German Microwave Conference*, 471–474, Mar. 2008.
21. Zhai, G. H., W. Hong, K. Wu, J. X. Chen, P. Chen, J. Wei, and J. L. Tang, "Folded half mode substrate integrated waveguide 3 dB coupler," *IEEE Microw. Wireless Compon. Lett.*, Vol. 18, No. 8, 512–514, Aug. 2008.
22. Wang, Z., X. Li, S. Zhou, B. Yan, R.-M. Xu, and W. Lin, "Half mode substrate integrated folded waveguide (HMSIFW) and partial H -plane bandpass filter," *Progress In Electromagnetics Research*, Vol. 101, 203–216. 2010.
23. Xu, F., K. Wu, and X. P. Zhang, "Periodic leaky-wave antenna for millimeter waves based on substrate integrated waveguide," *IEEE Trans. on Antennas and Propagation*, Vol. 58, No. 2, 340–347, 2010.
24. Russell, K. J., "Microwave power combining techniques," *IEEE Trans. on Microwave Theory and Tech.*, Vol. 27, 472–478, 1979.
25. Germain, S., D. Deslandes, and K. Wu, "Development of substrate integrated waveguide power dividers," *Canadian Conference on Electrical and Computer Engineering*, 1921–1924, May 4–7, 2003.